Recent off-axis volcanism in the eastern Gulf of Aden: Implications for plume-ridge interaction

Sylvie Leroy, Elia d'Acremont, Christel Tiberi, Clemence Basuyau, Julia
Autin, F. Lucazeau, Heather Sloan

Recent off-axis volcanism in the eastern Gulf of Aden: Implications for plume–ridge interaction

Sylvie Leroy [a,b,*], Elia d'Acremont [a,b], Christel Tiberi [c], Clémence Basuyau [a,b], Julia Autin [a,b], Francis Lucazeau [d], Heather Sloan [e]

[a] ISTeP, Univ Paris 06, Case 129, 4 place Jussieu, 75252 Paris Cedex 05, France
[b] ISTeP, CNRS UMR 7193, Case 129, 4 place Jussieu, 75252 Paris Cedex 05, France
[c] Géosciences Montpellier, France
[d] Institut de Physique du Globe, Paris, France
[e] Environmental, Geographic and Geological Sciences, Lehman College, CUNY, NY, USA

Evidence of anomalous volcanism is readily observed in the Gulf of Aden, although, much of this oceanic basin remains as yet unmapped. In this paper, we investigate the possible connection of the Afar hotspot with a major off-axis volcanic structure and its interpretation as a consequence of a the anomalous presence of melt by integrating several data sets, both published and unpublished, from the Encens–Sheba cruise, the Aden New Century (ANC) cruise and several other onshore and marine surveys. These include bathymetric, gravity, magnetic, magneto-telluric data, and rock samples. Based upon these observations, interpretations were made of seafloor morphology, gravity and magnetic models, seafloor age, geochemical analyses and tectonic setting. We discuss the possible existence of a regional melting anomaly in the Gulf of Aden area and of the probability of its connection to the Afar plume. Several models that might explain the anomalous volcanism are taken into account, such as a local melting anomaly unrelated to the Afar plume, an anomalously large volume of melt associated with seafloor spreading, and interaction of the ridge with the Afar plume. A local melting anomaly and atypical seafloor spreading prove inconsistent with our observations. Two previously proposed models of plume–ridge interactions are examined: the diffuse plume dispersion called pancaked flow and channelized along-axis flow. We conclude that the configuration and structure of this young ocean basin may have the effect of channeling material away from the Afar plume along the Aden and Sheba Ridges to produce the off-axis volcanism observed on the ridge flanks. This interpretation implies that the influence of the Afar hotspot may extend much farther eastwards into the Gulf of Aden than previously believed. The segmentation of the Gulf of Aden and the configuration of the Aden–Sheba system may provide a potential opportunity to study channeled flow of solid plume mantle from the plume along a segmented ridge and nearby continental margins.

1. Introduction

A significant proportion of the global mid-ocean ridge (MOR) system (up to 20%) is strongly influenced by the presence of nearby mantle plumes (Schilling, 1991; Ito and Lin, 1995). Mantle plume influence produces long-wavelength gradients of chemical and physical properties that extend up to thousands of kilometers along the ridge from the hotspot source (Ito et al., 2003). Proximity to hotspots is known to exert a strong influence on spreading rate and ridge morphology. Portions of the MOR influenced by a nearby hotspot usually are associated with shallower depths and thicker crust as determined from seismic and gravity studies (Schilling et al., 1983;

Ito et al., 1999; Canales et al., 2002). Most studies of ridge–hotspot interactions have focused on fully developed ridge systems but we have little information from relatively young, narrow ocean basins where large lateral variations of lithosphere thickness occur.

The slow-spreading ridges of the Gulf of Aden display several features that may are typical of ridge interaction with a mantle plume. At its westernmost end, the ridge is undeniably under the influence of the Afar plume (Tard et al., 1991; Hébert et al., 2001), but until now little evidence of surface expression of plume interaction in the eastern end of the Gulf has been detected. The influence of the Afar plume played a critical role in the formation and evolution of the Gulf of Aden (Bellahsen et al., 2003). Hébert et al. (2001) proposed the Shukra el Sheik fracture zone (SSFZ; Fig.1a) as the eastern limit of the Afar plume influence and corresponding major changes in the mechanical behaviour of the lithosphere. There is, however, some evidence that the Afar plume has also influenced the eastern domain.

* Corresponding author. ISTeP, CNRS UMR 7193, Case 129, 4 place Jussieu, 75252 Paris Cedex 05, France. Tel.: +33 1 44273408; fax: +33 1 44275085.

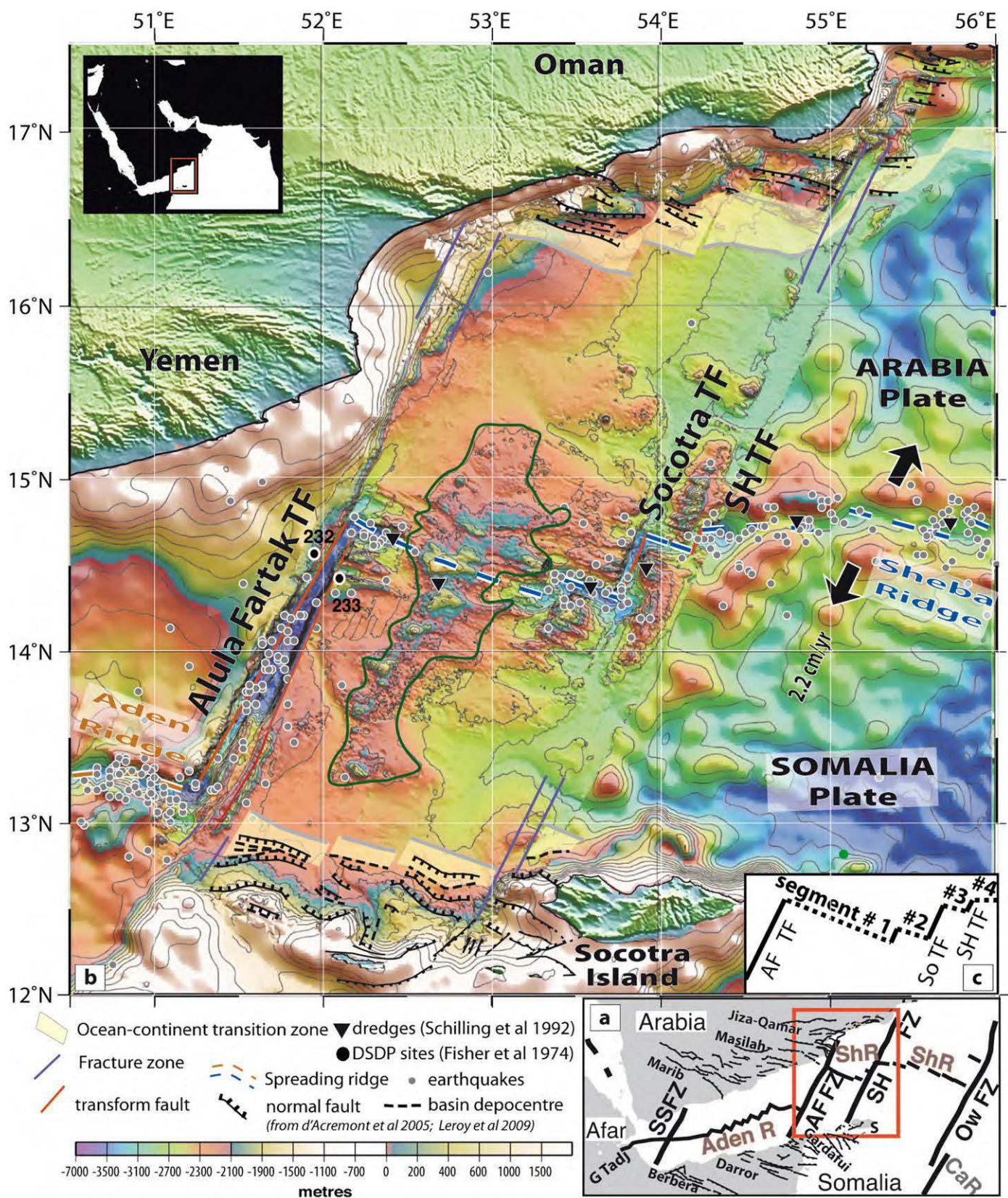E-mail address: sylvie.leroy@upmc.fr (S. Leroy).

Fig. 1. a — Schematic map of the Gulf of Aden and of the main Mesozoic grabens assembled by this study. G Tadj: Gulf of Tadjura; SSFZ: Shukra El Sheik Fracture zone; AFFZ: Alula Fartak Fracture zone; SHFZ: Socotra Hadbeen Fracture zone; OwFZ: Owen Fracture zone; Aden R: Aden Ridge, ShR: Sheba Ridge; CaR: Carlsberg Ridge; S: Socotra Island. b — Topographic and bathymetric map of the study area established with SRTM data (Farr and Kobrick, 2000) onland and multibeam bathymetry from the Encens–Sheba cruise between Alula Fartak and Socotra Hadbeen (SH) Transform faults (TF) (Leroy et al., 2004); and the compiled data from all cruises in the database of Smith and Sandwell (1997). Black arrows show relative plate motions (Fournier et al., 2001). The locations of the dredges (Schilling et al. 1992) and DSDP sites (Fisher et al. 1974) are indicated with black inverted triangles and circles, respectively. The major volcanic area is outlined in dark green. Although located on the highly magmatic segment 1, note that the dredges do not sample any of the volcanoes. c — Structural sketch of the Sheba Ridge and location of the spreading segments (Leroy et al. 2004).

2

Marine geophysical data (bathymetry, gravity and magnetization) were acquired during the Encens–Sheba cruise from the full width of the Gulf of Aden basin between the Alula Fartak and Socotra Hadbeen Fracture Zones (AFFZ and SHFZ, respectively). Data coverage extends from the northern continental margin to the southern one (Fig.1b; Leroy et al., 2004). Major off-axis volcanic structures (outlined in dark green in Fig. 1b) were observed and interpreted as the result of a melting anomaly or the anomalous presence of melt beneath the Gulf of Aden. Here, we examine the possibility that the source of this melt may be the mantle plume rising beneath Afar and that the Afar plume may influence much of Gulf of Aden region. The extensive integrated on shore and marine dataset allows interpretations of structure, character, and age determination. We discuss several models: a local melting anomaly unrelated to the Afar plume, atypical seafloor spreading, and two-end member models of plume–ridge interaction: diffuse flow (Ito et al., 1996; Ribe, 1996; Ito et al., 1997, 1999) and channelized along-axis flow (Vogt and Johnson, 1975; Vogt, 1976; Morgan, 1978; Sleep, 1996; Albers and Christensen, 2001). Finally, we propose channelized flow of material from the Afar hotspot along the Aden and Sheba Ridges to explain the presence of anomalous volcanism throughout the Gulf of Aden as far eastward as the longitude of 54°E.

2. Geodynamic setting of the Gulf of Aden

2.1. Opening of the Gulf of Aden

The Aden and Sheba Ridges within the Gulf of Aden define the southern boundary of the Arabian Plate. They extend from the Owen Fracture Zone (58°E) to the Gulf of Tadjoura where the Aden Ridge enters into the African continent (43°E) (Fig. 1; Manighetti et al., 1997). Continental rifting started 35 Myr ago with a direction of extension of approximately N20°E and culminated in seafloor spreading during the early Miocene (18 Ma) (e.g., Autin et al., 2010; d'Acremont et al., 2010) (20 Ma in the easternmost part; Fournier et al., 2008). Rifting re-activated pre-existing NW–SE to E–W Jurassic and/or Cretaceous basins (Platel and Roger, 1989; Ellis et al., 1996; Birse et al., 1997; Watchorn et al., 1998). The N75°E average orientation of the shores of the Gulf of Aden is 50° oblique to the present opening direction.

Regional plate kinematic models indicate that the Sheba Ridge is spreading at the rate of 2.2 cm/yr along a mean direction of N26°E (Fournier et al., 2001). The Gulf of Aden opened as the Carlsberg Ridge propagated NW until it reached the AFFZ, then WSW toward the Afar hotspot until it reached the mouth of the Gulf of Tadjoura (Manighetti et al., 1997; Courtillot et al., 1999). In the westernmost part of the Gulf, geophysical data (Audin et al., 2004) show clear evidence of present-day southwestward propagation of the ridge in the Gulf of Tadjoura toward the African continent. Magnetic timescale Chron 5c, which is well defined between the SSFZ and the AFFZ (Fig. 2), constrains the inception of seafloor spreading within the Gulf of Aden to 16 Ma at the latest (d'Acremont, 2002), a date confirmed by this study. East of AFFZ (Fig. 1), identification of Chron 5d yields an age of at least 17.6 Ma for the inception of seafloor spreading in the eastern part of the Gulf (Leroy et al., 2004).

2.2. Segmentation of the margins and ridge

The along-axis segmentation of continental margins created during the early stage of rifting was replaced by a new axial geometry of shorter segments during the late rifting stage (d'Acremont et al., 2005). This late stage segmentation persisted through the onset of seafloor spreading and evolved into the present-day ridge geometry (Leroy et al., 2004; d'Acremont et al., 2006). The configuration of the Sheba Ridge echoes the northern edge of a series of Mesozoic basins, now located on the Arabian Plate, and the Aden Ridge echoes the southern edge of the Mesozoic basins, now located on the African Plate (Fig. 1a; Bellahsen et al., 2006; d'Acremont et al., 2006).

The oceanic domain of the Gulf is divided into three parts by two major discontinuities: the SSFZ and the AFFZ (Figs. 1 and 2). The SSFZ has been proposed as the limit of the influence of the Afar hotspot and the location of a major change in the character of the lithosphere (Manighetti et al., 1997; Audin et al., 2001; Dauteuil et al., 2001; Hébert et al., 2001). The AFFZ separates the central and eastern parts of the Gulf (Tamsett and Searle, 1990). The westernmost oceanic domain presents a straight ridge without obvious segmentation whereas the Aden Ridge in the central domain is more highly segmented with seven transform faults that shift the ridge northwards by successive offsets ranging from 14 to 47 km (Fig. 2). The Aden Ridge is joined to Sheba Ridge by a 180 km offset of the Alula Fartak transform fault (AFTF).

2.3. The Afar plume

The Afar hotspot, located in the continental environment of the Horn of Africa in the west of the Gulf of Aden, is one of the most active hotspots in the world (e.g., Courtillot et al., 2003). The Afar plume volcanism has been extensively studied during the last decade (e.g., Hofmann et al., 1997). Fig. 2 presents a compilation of all published outcrop locations and ages in the study area.

In central eastern Afar, on the edge of the Ali Sabieh block (Fig. 2), radiometric ages of volcanic rocks range from 20 Ma to 10 Ma. In the same region, volcanic activity (stratoid basalt) dating from 4 Ma to present was reported by Audin et al. (2004). The high flood basalt plateaus in Ethiopia and Yemen are the signatures of voluminous eruptions developed as the result of one or two Paleogene mantle plumes (e.g., Ebinger and Sleep, 1998; George et al., 1998). A synthesis of $^{40}Ar/^{39}Ar$ data from these plateaus reveals basaltic and rhyolitic flood volcanism occurred from ~40 Ma to present, with the highest eruption rates at ~31 Ma (Fig. 2; Baker et al., 1996; Hofmann et al., 1997; Ukstins et al., 2002; Audin et al., 2004; Kieffer et al., 2004; Wolfenden et al., 2005).

Recent widespread volcanic events dated from 12 Ma to 10 Ma and 6 Ma to present span a 2500 km wide area in the Arabia plate from Northern and Central Arabia south and east to Yemen (e.g., Zumbo et al., 1995; Bertrand et al., 2003; Coulie et al., 2003). The volcanic activity in Arabia postdates the rifting of the Gulf of Aden and the onset of the oceanic spreading. A mantle type HIMU (high $^{238}U/^{204}Pb$) signature was recorded for this volcanism (Bertrand et al., 2003).

In the Gulf of Aden, basaltic flood volcanism occurred prior to, or perhaps coeval with, the initiation of rifting in the southern Red Sea (Bosworth et al., 2005; Wolfenden et al., 2005). This caused the formation of volcanic continental margins characterized by seaward dipping reflector sequences dated from 40 Ma to 16 Ma (Tard et al., 1991). The Plio-Quaternary magmatic segments in the Main Ethiopian Rift (MER) overprint earlier Red Sea–Gulf of Aden structures and mask eastern basin margins (Wolfenden et al., 2005).

In Somalia, Plio-Quaternary volcanic outcrops appear offshore in the Daban, Bosaso and Qandala Oligo-Miocene basins (Fig. 2), which correspond to the southern margin of the Gulf of Aden (Fantozzi and Sgavetti, 1998). Unfortunately, the accurate age and geochemistry of the Somali margin volcanism remains unknown.

Offshore, the DSDP leg 24 sites 231 to 233 recovered ash deposits Plio-Quaternary in age (Fisher et al., 1974). The ash deposits from the site 231 consist of microtephra that reveal three main pulses of volcanism at ca. 4.0–3.2 Ma, 2.4 Ma and 1.7–1.3 Ma, which correspond with peaks in volcanic activity in the Ethiopian Rift System (Feakins et al., 2007). In addition, dredges along the mid-ocean ridge axis have recovered basalts with OIB (oceanic island basalts) type geochemical characteristics (Schilling et al., 1992) from the mouth of the Gulf of Tadjoura as far east as 46.5°E (Orihashi et al., 2003). East of 48°E, the geochemical signature of the Aden and Sheba Ridges is found to be
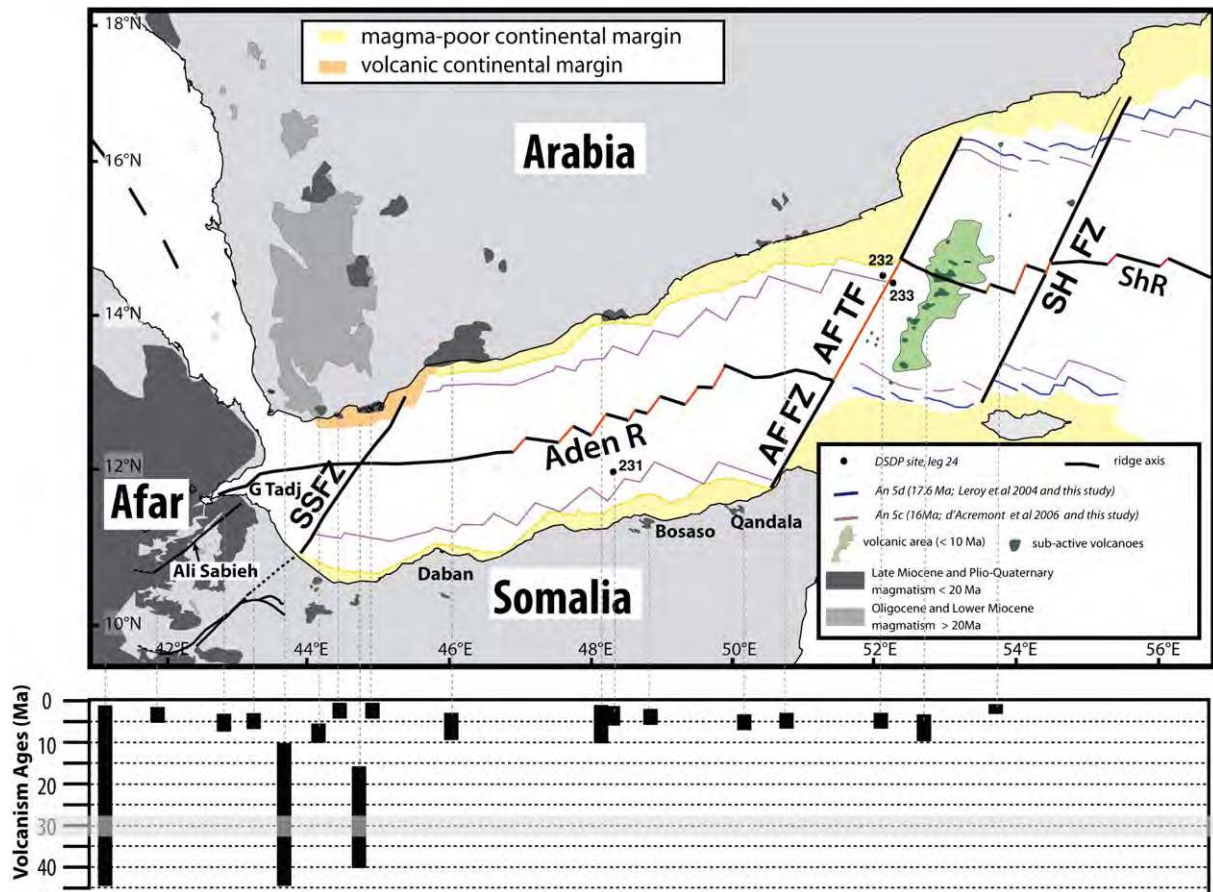
Fig. 2. Simplified map of the main outcrops of magmatic rocks (on- and offshore) and their associated ages in the Gulf of Aden area compiled from Zumbo et al. (1995); Baker et al. (1996); Hofmann et al. (1997); Fantozzi and Sgavetti (1998); Ukstins et al. (2002); Bertrand et al. (2003); Coulie et al. (2003); Orihashi et al. (2003); Audin et al. (2004); Bosworth et al. (2005); Pik et al. (2006); Feakins et al. (2007); Lucazeau et al. (2009); Autin et al. (2010). The age of ~30 Ma, which was determined by Hofmann et al. (1997) to correspond to the main volcanic episode of the Afar hotspot, is highlighted in light grey in the plot of volcanism ages in the lower part of figure. The isochrons are published in part by d'Acremont (2002); Leroy et al. (2004); d'Acremont et al. (2006, 2010) with the remainder coming from this study. Bold solid lines striking N30°E = SSFZ: Shukra el Sheik Fracture Zone — AFFZ: Alula Fartak Fracture Zone — SHFZ: Socotra Hadbeen Fracture Zone. Red lines: transform faults and AFTF: Alula Fartak transform fault — ShR: Sheba Ridge — Aden R: Aden Ridge.

DUPAL-like (depleted asthenosphere) and is considered by Schilling et al. (1992) to be uninfluenced by the Afar plume. This suggests that the eastward extent of the Afar plume influence on mantle composition may be 46.5°E. However, it should be noted that the volcanoes on the flanks of the Sheba Ridge have never been sampled by dredging (Fig. 1).

Geochemical analyses have revealed anomalously high $^3He/^4He$ ratios in Afar and mantle type HIMU signatures along the northern margin of the Gulf of Aden. $^3He/^4He$ ratios may be used to unequivocally determine the origin of the volcanism (Pik et al., 2006). The $^3He/^4He$ ratios from Afar are as high as 20 Ra, which is characteristic of undegassed mantle material interpreted to have originated from the "deep mantle" and is probably related to a plume beneath Afar (Pik et al., 2006). Unfortunately, this type of chemical analyses is not available along the ridge or from the anomalous volcanic features on its flanks. The HIMU signature along the Gulf of Aden margin while indicative of a mantle melt source, does not necessarily indicate that the melt came from the Afar mantle plume. However, it may reflect a heterogeneous composition due to interaction of plume material with the Arabian Plate continental lithosphere (Bertrand et al., 2003). Observations at other ridges near hotspots effectively show a decrease in the distance of along-axis plume influence with increasing plume–ridge separation until the influence becomes insignificant at distances more than ~500 km (Ito and Lin 1995; Ribe et al., 1995; Ito et al., 2003). However, several exceptions to this tendency have been noted. For example, the Kerguelen/La Réunion hotspots still exert a residual influence on the

Central and Southeast Indian ridges. These ridges are at more than 1000 km from the hotspots (Mahoney et al., 1989; Graham et al., 1999).

Mantle seismological studies of the Afar area indicate the existence of very low velocity zones below this region, both at local and regional scales (e.g., Gurnis et al., 2000; Debayle et al., 2001). The observed velocity anomalies suggest a significant melt fraction is present in the upper mantle (e.g., Bastow et al., 2005; Benoit et al., 2006). Yet, the spatial extent and location of the plume, as well as its connectivity to a lower mantle anomaly imaged in global seismic models is still debatable (Ritsema and van Heijst Hendrik, 2000; Montelli et al., 2006; Simmons et al., 2007). Several authors document a zone of low velocity beneath Ethiopia, the Red Sea, and much of the southern Arabian Peninsula (Bastow et al., 2005; Benoit et al., 2006). Absolute S-wave delay times relative to a standard Earth model are some of the largest worldwide, suggesting a significant melt fraction within the upper mantle (Park et al., 2007). It has been suggested that the low velocity mantle zone beneath western Saudi Arabia could be caused either by migrating material from the Afar plume (Park et al., 2007; Simmons et al., 2007), upwelling mantle material associated with Red Sea rifting, or small-scale local convection (Hansen et al., 2007). A more recent study found a zone of anomalously slow shear wave velocity between the Afar hotspot and the Gulf of Aden up to 55°E longitude at depths shallower than 150 km, suggesting that the Afar upwelling may be feeding the Gulf of Aden ridge system at the base of the lithosphere (Sicilia et al., 2008).

In addition, several lines of geophysical evidence indicate that a melt anomaly associated with the Afar mantle plume may still exist. Anomalously low S-wave velocities in the upper mantle were recorded beneath the MER and Afar at depths of ~30 and 400 km, implying the presence of partial melt (Knox et al., 1998). Seismic tomography images a low velocity zone rising from the core–mantle boundary beneath South Africa and propagating towards the northeast to reach the base of the lithosphere beneath East Africa (Ritsema and van Heijst Hendrik, 2000). More recently, a tomographic study carried out by Montelli et al. (2006) suggested a very deep origin of the Afar plume.

3. The oceanic domain of the eastern Gulf of Aden (between AFFZ and SHFZ)

3.1. Bathymetric data

Full bathymetric coverage of the oceanic domain between longitude 52°E and 54°15E during the Encens–Sheba cruise (Fig.1b) reveals the morphology of the spreading ridge with four second order segments designated 1 to 4 in the following discussion. Segment 1 (Fig. 1c) is atypically long, measuring 120 km, and display unusual morphology. The three other segments have typical slow-spreading axial valleys (Thibaud et al., 1998). Segment 2 is 40 km long and located west of the Socotra transform fault (SoTF; Fig. 1c). Segment 3 is 30 km long and located east of that fault. Segment 4 is 30 km long and located east of the SHTF. The strike of the axis changes from segment 3 (N110°E) to segment 4 (N90°E) (Fig. 1b). Large nodal basins occur on either side of each axial discontinuity; the deepest (3750 m) and largest one is located at the intersection between the ridge axis and the SoTF.

At 1000 m depth, the segment 1 axial domain is anomalously shallow for a mid-ocean ridge, particularly a slow-spreading one. Rather than the typical fault-bound, deep axial valley found at most slow-spreading ridges, the axial domain of segment 1 is domed at the segment center with fault scarps forming the walls of a deep valley only at the segment ends (Fig. 1b). Deformation is diffuse at the segment ends and becomes more focused toward the segment center in such a way that the segment has the form of an hourglass typical of slow-spreading ridges (Sempéré et al., 1993). The bathymetric data reveals peculiar seafloor morphology on the flanks of segment 1 that differs from the other 3 segments; both the flanks and the axial valley are marked by large nearly circular volcanic domes. Most of the domes have diameters of 1–2 km, but some are 5–10 km in diameter (Figs. 1b and 3). Many of these volcanoes present well-developed calderas (Figs. 1b and 3; Leroy et al., 2004). These volcanic constructions are

well-developed 140 km south of the axis where their heights reach ~700 m above sea floor (Figs. 3 and 4). Moreover, four small volcanoes, not included in the mapped volcanic area, lie nearby the AFTF (Fig. 3). Similar volcanic edifices also exist on the northern flank up to 80 km from the axis, but they are less prominent (400 m above sea floor, Figs. 3 and 4). Although higher sediment inflow from Yemen may have partially buried the northern volcanic structures (Platel and Roger, 1989; d'Acremont et al., 2005), there nevertheless appears to be a clear asymmetry in the distribution of volcanic features between the northern and southern flanks (Figs. 1b, 3–5). The extent of the volcanoes on the northern flank is broader in the axis-parallel direction and narrower in the direction perpendicular to the axis when compared to the southern flank (Fig. 5). These aspects of the seafloor surface morphology may be associated with deeper structural features.

3.2. Gravimetric data

We use free air anomaly data from the Encens–Sheba (Leroy et al., 2004) and Encens (Leroy et al., 2006, submitted for publication) cruises. The effect of a constant thickness (6 km), constant density (2.750 g cm^{-3}) crust was removed from the free air anomaly to obtain mantle Bouguer anomaly (MBA) values. Residual mantle Bouguer anomaly (RMBA) corresponds to the MBA corrected for the density variations related to the cooling with age (i.e., distance from the ridge axis). RMBA lows correspond to thicker constant density model crust or to lighter material, whereas RMBA highs correspond to thinner constant density model crust or to denser crustal material (see Leroy et al., 2004; d'Acremont et al., 2006, 2010).

There is a large asymmetric negative RMBA (−220 to −270 mGals) extending across the flanks of segment 1 parallel to the direction of spreading (SSW–NNE; Fig. 6). In the axis-parallel direction, the RMBA values vary ~70 mGals between the segment center and the segment ends. There is a corresponding 2 km variation in depth of the axial valley floor of the segment (Fig. 1b). This variability of RMBA and axial depth between the center and the ends of segment 1 is greater than that measured for any other slow-spreading ridge segment worldwide (Leroy et al., 2004; d'Acremont et al., 2010). A clear asymmetry between the northern and southern flank also appears in the gravity data, with RMBA values lower on the northern than in the southern flank. The most negative RMBA value (−280 mGals) occurs beneath the prominent volcano on the southern flank (latitude N13°20′; single arrows in Figs. 4–6). In addition, low negative RMBA (about −270 mGals) are observed to the west of the most negative RMBA (double arrows in Fig. 6).
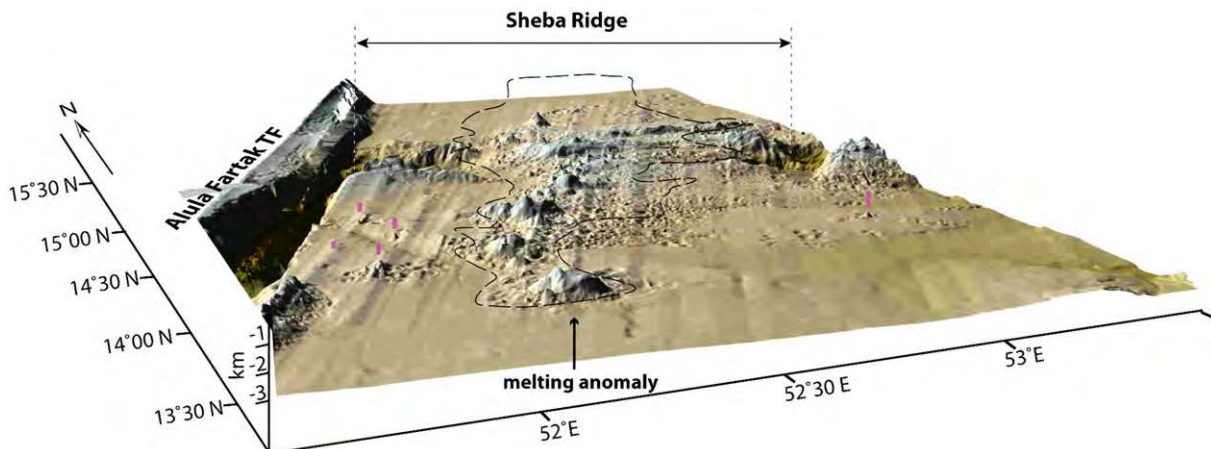

Fig. 3. Three dimensional view of the volcanic area southern of the Sheba Ridge, highlighted by a dashed line. Small isolated volcanoes are indicated by vertical dark rose lines.
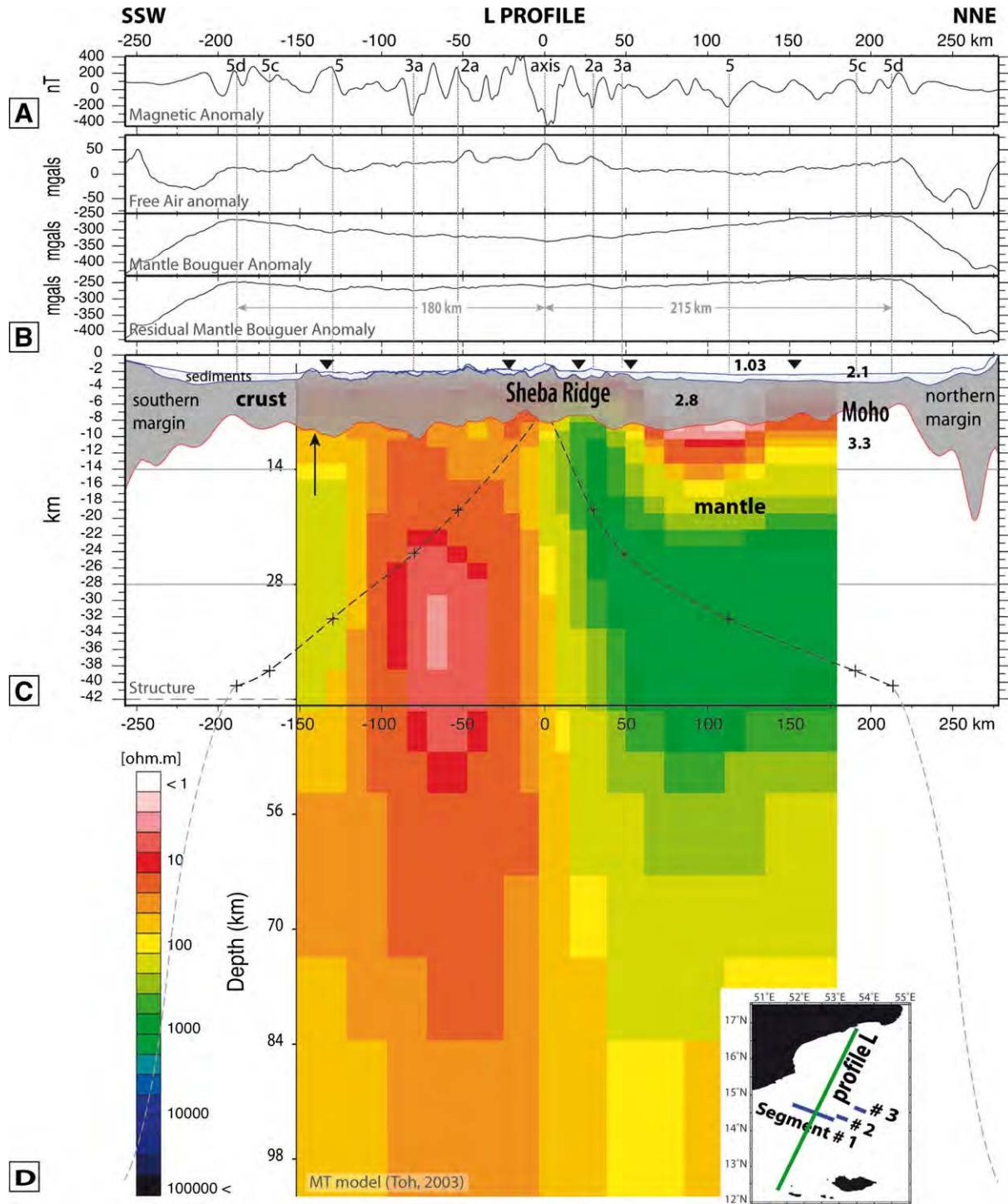
Fig. 4. Profile L of Encens–Sheba cruise striking SSW–NNE and crossing segment 1 of the Sheba Ridge. See inset map for location of the profile. A — magnetic anomaly profile and magnetic anomalies identified by Leroy et al. (2004) and d'Acremont et al. (2006, 2010). B — gravity data from top to bottom: observed free air anomaly, computed Mantle Bouguer and Residual Mantle Bouguer anomalies (see Fig. 6 for parameters and method of computation). C — simplified crustal section computed by gravity modeling using average densities of 1.03, 2.1, 2.75 and 3.3 g cm^{-3} (water, sediment, crust and mantle, respectively (d'Acremont et al., 2006, 2010)). The solid arrow is located at the melting anomaly. Simplified lithospheric thickness computed by assuming a half-space cooling model for each age of the oceanic crust with the base of the lithosphere defined by the 1300 °C isotherm surface indicated by a dashed line with +'s (Renkin and Sclater, 1988; Turcotte and Schubert, 1982). The +'s mark the locations that correspond with identified isochrons at the seafloor surface. D — electrical resistivity model from ANC cruise (Tamaki and Fujimoto, 2001). Methods of computation are published by Toh (2003). Inverted triangles are the locations of the Ocean Bottom ElectroMagnetometer (OBEM).

3.3. Magnetic data

Previously interpreted magnetic data from Encens–Sheba cruise (Leroy et al., 2004; d'Acremont et al., 2006) are buttressed by newer data from Encens cruise (Leroy et al., 2006, submitted for publication) and Encens-Flux cruise (Lucazeau et al., 2008). We present here identifications of Chron 0, 2a, 3a, 4a, 5, 5c and 5d (Fig. 5) from the new magnetic data which has been compiled and interpreted in part by d'Acremont et al. (2010). The oldest magnetic anomaly identified is Chron 5d on either side of the spreading ridge at foot of the northern and southern continental margins (Figs. 4a and 5). The northern flank of the Sheba Ridge is wider than its southern flank (about 215 km and
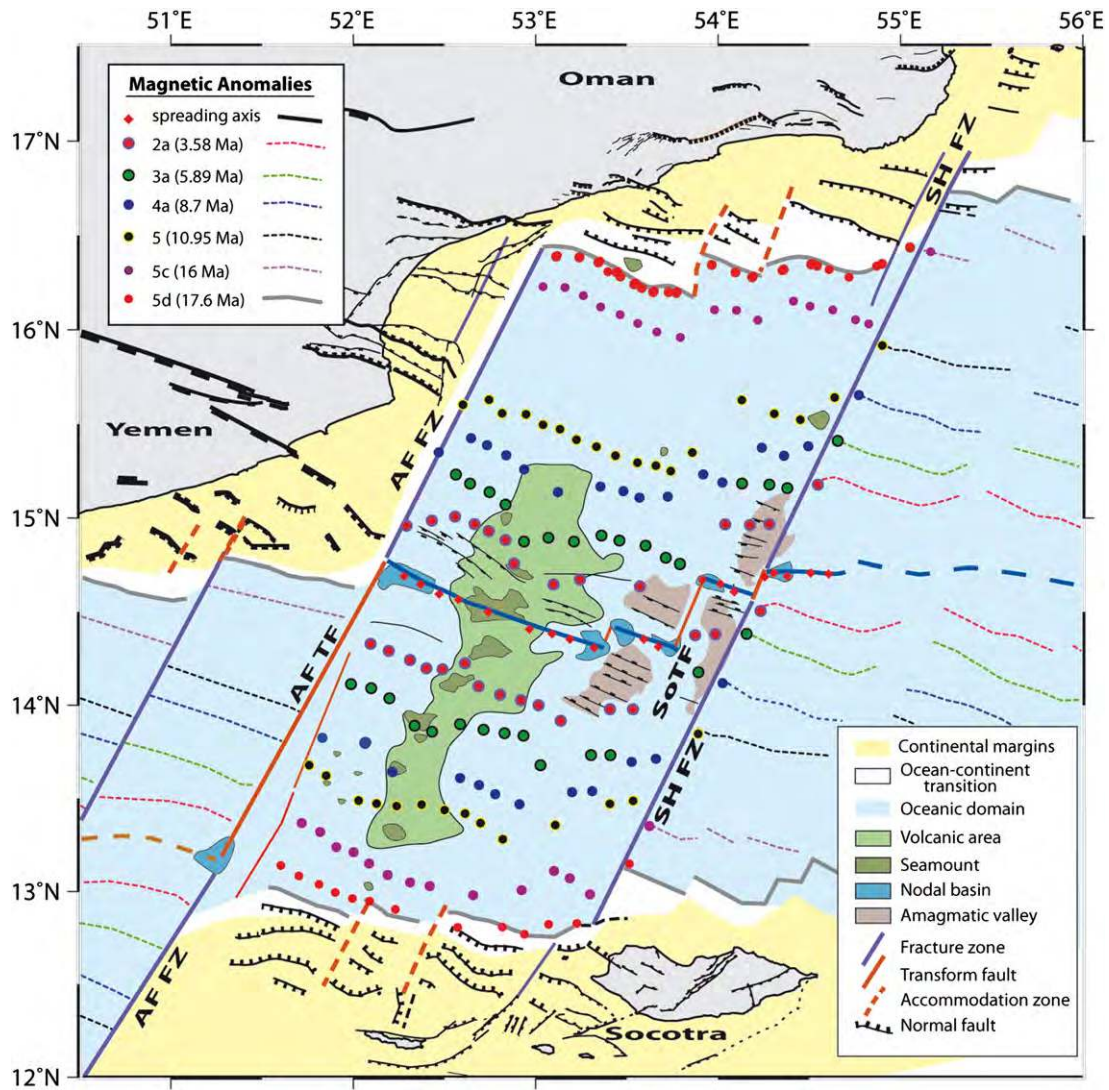
Fig. 5. Structural schematic of the area of volcanic features. The continental margins map is from d'Acremont et al. (2005). Volcanoes are highlighted in dark green as well as the topographic bulge (green surface extending to 12,000 km^2). Note the perturbations of the magnetic anomalies in both flanks from A5 time for the southern and after A5 time for the northern one. SoTF: Socotra Transform fault; AFTF: Alula Fartak Transform fault; SHFZ: Socotra Hadbeen Fracture zone. Magnetic anomaly identifications are from d'Acremont et al. (2006, 2010) and the isochrons from this study. The structural schematic is developed from d'Acremont et al. (2005); Bellahsen et al. (2006); Autin et al. (2010) and this study.

180 km, respectively). Profile L oriented NE–SW and extending from the southern margin to the northern one illustrates this asymmetry between the northern and southern oceanic domains in terms of basin width, depth and crustal and lithospheric thicknesses (Fig. 4). This asymmetry is associated with a ridge jump near the volcanic area at Chron 5 time (10 Ma; Fig. 5; Leroy et al., 2004; d'Acremont et al., 2010). The magnetic anomalies are well defined on the northern flank in most of the across-axis profiles (Fig. 4a), but appear to be disrupted on the southern flank in the area of at the volcanic features. On the southern flank, Chrons 0 to 5 appear to be disrupted within the zone of volcanism (Fig. 5). Disruption of Chron 2a and 3a appears in the northern flank within the zone of volcanoes. As the isochrons are not disrupted outside of the major volcanic area, their sinuous configuration may indicate "overprinting" of the original magnetization by volcanic activity.

3.4. Electro-magnetic data

Fig. 4d shows the cross-section of lithospheric electrical resistivity (Toh, 2003), which displays a low resistivity domain located below the southern flank of the Sheba ridge at depths ranging from 20 to 50 km, below the theoretical lithosphere (dashed line on Fig. 4d). This anomaly of low resistivity coincides with bathymetric and gravimetric anomalies of the southern flank. High temperatures, the presence of partial melt and/or the presence of water could cause this decrease in the electrical resistivity (Toh, 2003; Constable and Heinson, 2004).

3.5. Seismologic data

Segment 1 of the Sheba Ridge is marked by a lack of seismicity with respect to the other segments of the ridge (Fig. 1b). This could be related to the presence of the volcanic area and of associated melting at depth. Such a melting anomaly is evoked by several seismological studies outlined below. Surface waves velocity minima were observed beneath the Afar hotspot, the Red Sea, Gulf of Aden, and locally between AFFZ and SHFZ at about 100 km depth (Sebai et al., 2006). Partial melting (3% to 6%) at a depth of between 60 and 200 km beneath the northern margin in the Southern Oman area along the prolongation of the AFFZ and the SHFZ is indicated by joint inversion of gravity and teleseismic data (Basuyau et al., 2010). These results point to the presence of unusually hot asthenospheric material at least in the north of the study area (Basuyau et al., 2010). Unfortunately,
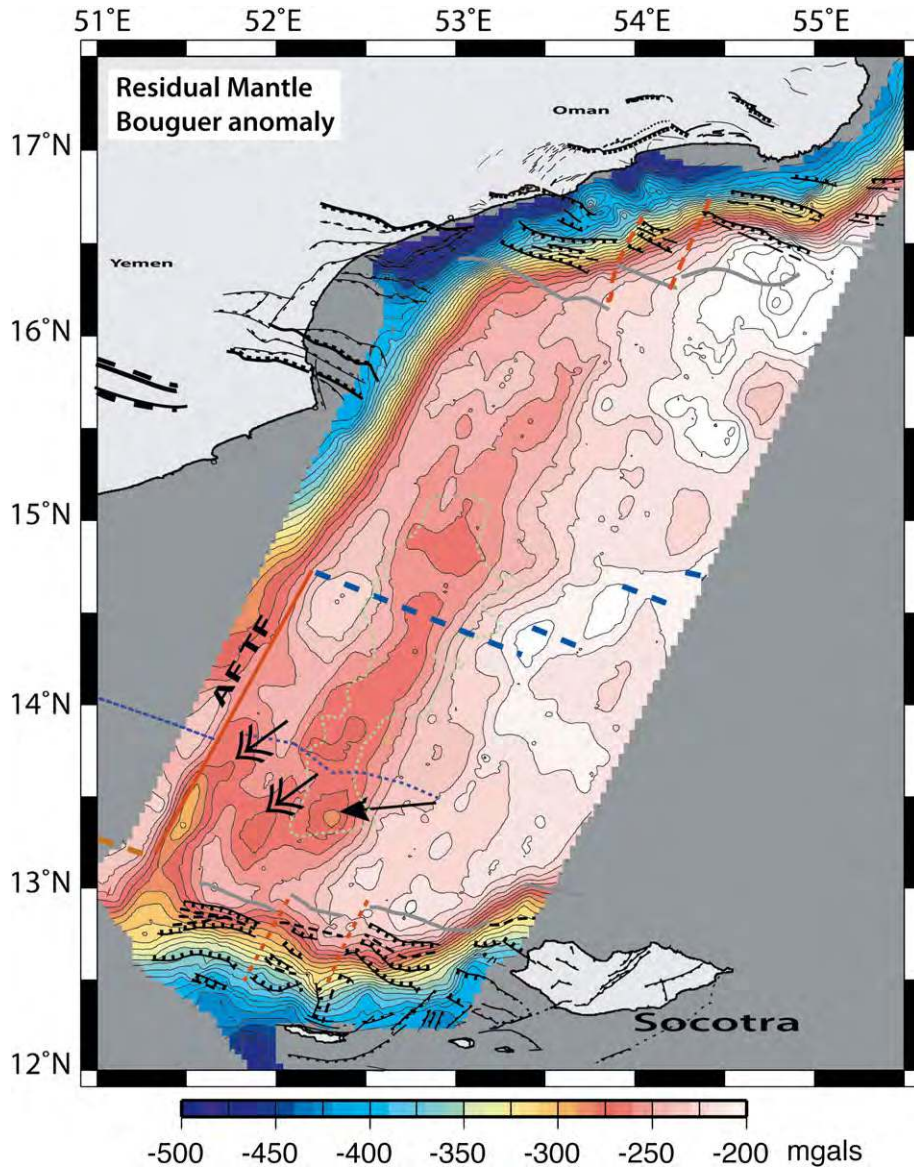
Fig. 6. Residual Mantle Bouguer map of the Encens–Sheba cruise area (contour interval is 10 mGals) computed from a model with a constant crustal thickness of 6 km, average densities of 1.03, 2.1, 2.75 and 3.3 g cm^{-3} (water, sediment, crust and mantle, respectively). The gravity and thermal effect of the model is computed with a multilayer method using a fast Fourier transform technique that is fully 3-D (for explanation of the method see d'Acremont et al. (2006, 2010)). The four ridge segments (1 to 4) are marked in dashed solid lines as well as the Aden R in orange. The red line corresponds to the AFTF, the dashed green line to the major volcanic area and the dashed blue line to the isochron 4a. The structural schematic is taken from Leroy et al. (2004); d'Acremont et al. (2005) and this study. Arrow indicates the location of the lower Residual Mantle Bouguer Anomaly interpreted as the melting anomaly. Double arrows indicate the low RMBA in the east of the AFTF.

little seismic data, which might constrain mantle structure, has been collected from the southern part of the area (Tiberi et al., 2007).

3.6. Heat flow and multichannel seismic data

In the same area between AFFZ and SHFZ, at the foot of the northern continental margin, high heat flow (~ 900 mW/m^2) has been observed over a volcano imaged by multichannel seismic data in the transitional domain of the segment 1 (Leroy et al., 2006; Autin et al., 2010; Figs. 2 and 5). The highly reflective and thick horizons near the volcano are interpreted as lava flows or sills interstratified with sediments. As they are overlain by post-rift sediments, which deformed progressively with time, the likely period of activity for this volcano started at the beginning of the spreading and continued during post-rift (Autin et al., 2010). The heat flow model of Lucazeau

et al. (2009) suggests that this volcano was active as recently as $\sim 100,000$ yr.

4. Discussion

Observations made in the zone between AFFZ and SHFZ suggest that the off-axis volcanic area may be related to anomalous presence of melt beneath the lithosphere. Based upon the extent of the associated seafloor bulge and its probable relationship to the thermal effect of this inferred melting zone, we estimate that the melting anomaly affects an area of at least 12,000 km^2 (Figs. 3 and 5). In support of this estimate, our observations in combination with those of other investigators, strongly suggest anomalously high asthenospheric temperatures beneath thin lithosphere near the ridge axis since the initiation of seafloor spreading. Geophysical and

geochemical analyses lend support to the interpretation of recent and ongoing magmatic activity and in the Gulf of Aden as far east as longitude 54°E.

A possible and tempting interpretation is that there is a connection between the melting anomaly and the Afar plume upwelling, but alternative models must be considered as well. One such model is a local melting anomaly unrelated to Afar, but fixed within the mantle. A second is a local melt source associated with the newly established seafloor spreading system. Finally, interaction of the Afar plume with the ridge system is examined. Two-end members of plume dispersion must be considered: a diffuse plume flow model and channeled flow along the ridge fed by Afar plume upwelling.

4.1. Presence of a local melt source unrelated to the Afar plume

Based upon the geophysical evidence, we believe that a melting anomaly exists beneath the prominent volcanoes on the southern flank of the Sheba Ridge between the AFFZ and SHFZ. This is the location of the most negative RMBA (Fig. 6), the largest electrical resistivity anomaly (P0 location in Fig. 7), and unusual seafloor morphology. As for many other mantle melt sources, this source may be considered fixed within the mantle, beneath the drifting plates above. Absolute plate motion reconstructions of Arabia and Somalia Plates (Müller et al., 1993) allow us to test the hypothesis of a local melt source. If this hypothesis is correct, the time of onset of volcanism and the track of volcanic activity on the plates as they drift over the melt source should match observations.

Currently the southern flank of the ridge resides above the mantle source at the point labeled P0 in Fig. 7. Based on absolute plate motion, the reconstructed track of the anomaly from present (P0) to 16 Ma (P5c) is drawn relative to the present-day plate geometry on the map (Fig. 7; red line) and retrospectively on the reconstructed map. The magnetic anomaly identifications were published in part by d'Acremont et al. (2010) and the rest are part of this study. If melting began as early as Chron 5c time (16 Ma), then we would expect a morphological footprint on the seafloor along the track as the plates drifted over the mantle source anomaly. At the time of the Chron 5c

(16 Ma), the southeastern Oman margin would have been located above the mantle source (location P5c in Fig. 7). At Chron 5 time (10 Ma), the Sheba Ridge would have drifted over the mantle source (location P5 in Fig. 7). If the appearance of the mantle source was associated with the onset of seafloor spreading (18 Ma), we would expect to see an oblique line of volcanoes or enhanced volcanism extending from the northern continental margin, through segments 4, 3 and 2 and across the flanks of segment 1 during the period from Chron 5c to Chron 3a (from 16 to 6 Ma). The red line in Fig. 7 describes a path similar to the expected volcanic trace for this case. But no evidence of such volcanic line appears in the seafloor morphology. Only isolated volcanoes are visible on the northern flank in the bathymetric map (Figs. 1b, 3 and 5). Therefore, if the mantle source is present, onset of associated volcanic activity could only have occurred after the time of Chron 5, i.e., younger than 10 Ma with the greatest activity taking place from 6 Ma to present (Chron 3a to 0). This deduction is supported by the disruptions of isochrons 5 to 0 observed in the southern flank and isochrons 3a and 2a in northern flank (Fig. 5). Nevertheless, the earliest volcanism in the eastern part of the region is known to have begun immediately after rifting, during the onset of spreading at about 17.6 Ma. It occurred at the edge of the continental margin in the ocean–continent transitional domain aligned with the area between AFFZ and SHFZ (Lucazeau et al., 2009; Autin et al., 2010). In the western region, the volcanic continental margins date from 40 Ma up to 16 Ma (Tard et al., 1991). Because volcanic activity in the region began earlier than 10 Ma, it is unlikely that the observed volcanism is the result of a fixed mantle source. Two other possible explanations may be considered: a source associated with the newly established ridge system or interaction of the ridge with the Afar plume.

4.2. Local source associated with the spreading ridge system

Segment 1 of Sheba Ridge presents features typical of the presence larger than normal melt supply, in particular, elevated axial depth and unusual RMBA (Figs. 1b, 3 and 4). Similar observations of elongated seamount chains and negative RMBA observed at others spreading
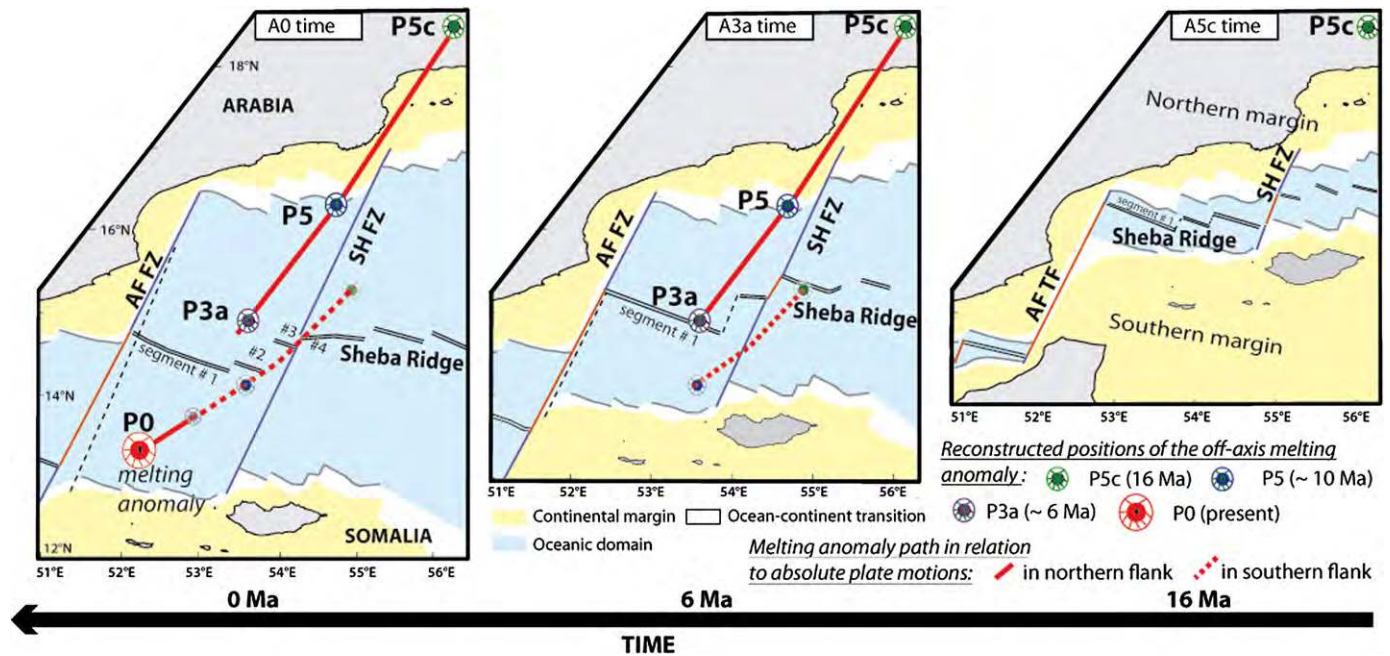

Fig. 7. Computed motion of the melting anomaly and tracks over time (from P0 location = red circle to P5c location = green circle) by using absolute plate motion reconstruction of Arabia and Somalia (Müller et al., 1993). In this sketch, we consider the present location as fixed and the direction of absolute plate motion is toward the northeast. Tracks of the mantle source on the plates are plotted tracing the location of the melting anomaly beneath the plate for each given time (red line). The dashed red line represents the track if the melting anomaly were beneath the southern plate before the 3a time. AFTF: Alula Fartak Transform fault (thin red line); AFFZ: Alula Fartak Fracture zone and SHFZ: Socotra Hadbeen Fracture zone (thin blue lines).

segments have been linked to the effect of fracture zones (e.g.,segment OH1, Mid-Atlantic Ridge, and Oceanographer FZ (Hooft et al., 2000; Rabain et al., 2001)). The steep mantle isotherms caused by the long offset transform are proposed to result in a focusing of melting at the segment center (Gregg et al., 2007). The AFTF could have had this effect on the segment 1 melt supply from the onset of spreading. However, recent effects of the melting anomaly are observed at not only the spreading axis, but also are evident in the recent volcanism at the edge of the AFTF that extends across the entire width of the Gulf of Aden near segment 1. Although, the effect of the long offset AFTF is a likely explanation for observations at the axis, it cannot explain evidence of anomalous volcanism on the flanks. We, therefore, consider that the long offset of the AFTF may contribute to the observed effects, but is minor in comparison with the potential contribution of mantle plume–ridge interaction.

4.3. Regional Afar plume–ridge interaction

Hotspot–ridge interaction is known to exert a long-wavelength influence on ridge bathymetry with shoaling toward axis-centered or near-axis plume sources observed in many locations (e.g., Ito et al., 2003). In all cases, the RMBA exhibit the very low values similar to those found at the Sheba Ridge. Our geological and geophysical observations of the Gulf of Aden suggest plume–ridge interaction. Fig. 8 shows two possible scenarios for the transport of plume material given the ridge geometry of the Gulf of Aden: (1) diffuse plume dispersion (Fig. 8a) as suggested by the numerical modeling in which plume material spreads radially like a "pancake" beneath the lithosphere (Ribe et al., 1995; Ribe, 1996; Ito et al., 1997, 1999) and

Fig. 8. Conceptual sketch of the off-axis melting anomaly radiating from the western part of the Gulf of Aden to east of the AFFZ. A — Diffuse plume dispersion at a depth below the onset of melting for the Gulf of Aden. The dark orange corresponds to the possible plume conduit and the orange shading to the location of the Afar plume from Sicilia et al. (2008). The light orange shading shows the dispersal of plume material encompassing the mapped volcanic area. Arrows indicate plume dispersal direction. B — Schematic illustration of the channelized along-axis Afar plume dispersion from west to east of the Gulf of Aden. Arrows indicate mantle flows directed from the plume to the Aden Ridge and subsequent along-axis dispersion at depths within a partial melting zone.

(2) channelized along-axis flow (Fig. 8b) where the mantle plume material moves along the Aden and Sheba Ridges as proposed by conceptual models of plume–ridge interaction (e.g., Vogt, 1971; Schilling et al., 1985; White et al., 1995) and by fluid dynamic calculations that suggest channeling of plume material for low spreading rates and very low viscosity plumes (Albers and Christensen, 2001). These two-end member models of plume flow (diffuse flow and channeled flow) have been explored at several locations where mantle plumes interact with ridges (e.g., Iceland, Kerguelen, Marion, Easter). The Gulf of Aden may provide a contrast to previously studied plume–ridge interaction systems.

In the case of the diffuse flow model (Fig. 8a), plume upwelling is vertical to some depth below the region of partial melting above which the plume spreads radially. For the Afar plume this region might correspond to the low velocity anomaly imaged by Sicilia et al. (2008). It has been proposed that the style of plume–ridge interaction may depend on ridge geometry (Georgen et al., 2001). In the case of small transform offsets, such as the small offsets of Aden Ridge transform faults, the plume width determines the extent or length of the ridge affected by the plume as demonstrated by Georgen et al. (2001). For highly segmented geometry with long transform offsets, such as the long offset of the AFTF on the Sheba Ridge, the extent of plume influence may be interrupted by displacement of the ridge beyond the plume's extent (Georgen et al., 2001). In the case of the Gulf of Aden, the plume is centered at or near the spreading axis at the westernmost end of the ridge system. In order for the observed volcanism on the flanks of the Sheba Ridge to be the result of diffuse plume flow, the flow would have to extend from Afar to at least as far as the volcanoes (Fig. 8a). In which case the width of the plume would be as great as 3000 km (radius of 1500 km). Although there is clear evidence of a melting anomaly within the restricted area between AFFZ and SHFZ and observations of volcanism in several area of the Gulf of Aden, regional doming, shallow bathymetry and widespread volcanism that would be caused by a 3000 km wide plume are not present, indicating that radial diffuse flow of the Afar plume is not a likely source for the volcanism on the ridge flanks at 54°E.

The channelized along-axis plume flow model proposes mantle flow directly from plume along the ridge axis within or above the melting zone beneath the spreading axis (Georgen et al., 2001; Fig. 8b). Offsets of the ridge axis at transform faults may have a damming effect on this flow due to the rheological barriers they constitute for the along-axis plume dispersion (Vogt and Johnson, 1975; Schilling et al., 1982). Indeed, abrupt changes of along-axis plume flow at fracture zones are indicated at many plume–ridge systems (e.g., Iceland/Charlie Gibbs Fracture Zone (Vogt and Johnson, 1975); Discovery/Agulhas Fracture Zone (Douglass et al., 1995); Amsterdam–St. Paul/Zeewolf transform (Graham et al., 1999)). Although the Afar plume may be considered as a ridge-centered plume similar to Iceland, the tectonic setting of the Gulf of Aden makes for significant differences between the Afar/Aden–Sheba system and others plume–ridge systems that have been studied.

The Gulf of Aden is a narrow oceanic basin (50 km in the west of SSFZ, 300 km up to AFFZ, and 400 km in the east of AFFZ) that has a low spreading rate (11 mm/yr) and is confined between blocks of relatively thick continental lithosphere (Fig. 9a). These conditions favor channeled flow. Conditions within the Gulf of Aden are particularly important because channeled flow implicitly invokes significant variations in lithospheric thickness with distance from the ridge axis. Such lithospheric thickness variations may even be required to create a sloping rheological boundary layer that focuses plume material along the ridge axis and inhibits its flow away from the ridge axis (Albers and Christensen, 2001). Changes in rock rheology due to dehydration during melting may affect plume–ridge interaction by reducing or negating the slope of the base of the lithosphere, creating a uniform horizontal viscous lid beneath the lithosphere (Hirth and Kohlstedt, 1996). This effect, proposed for
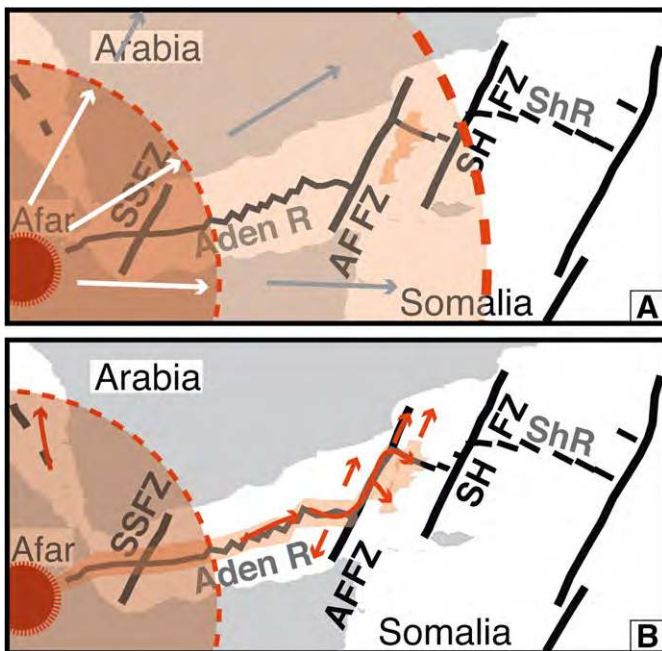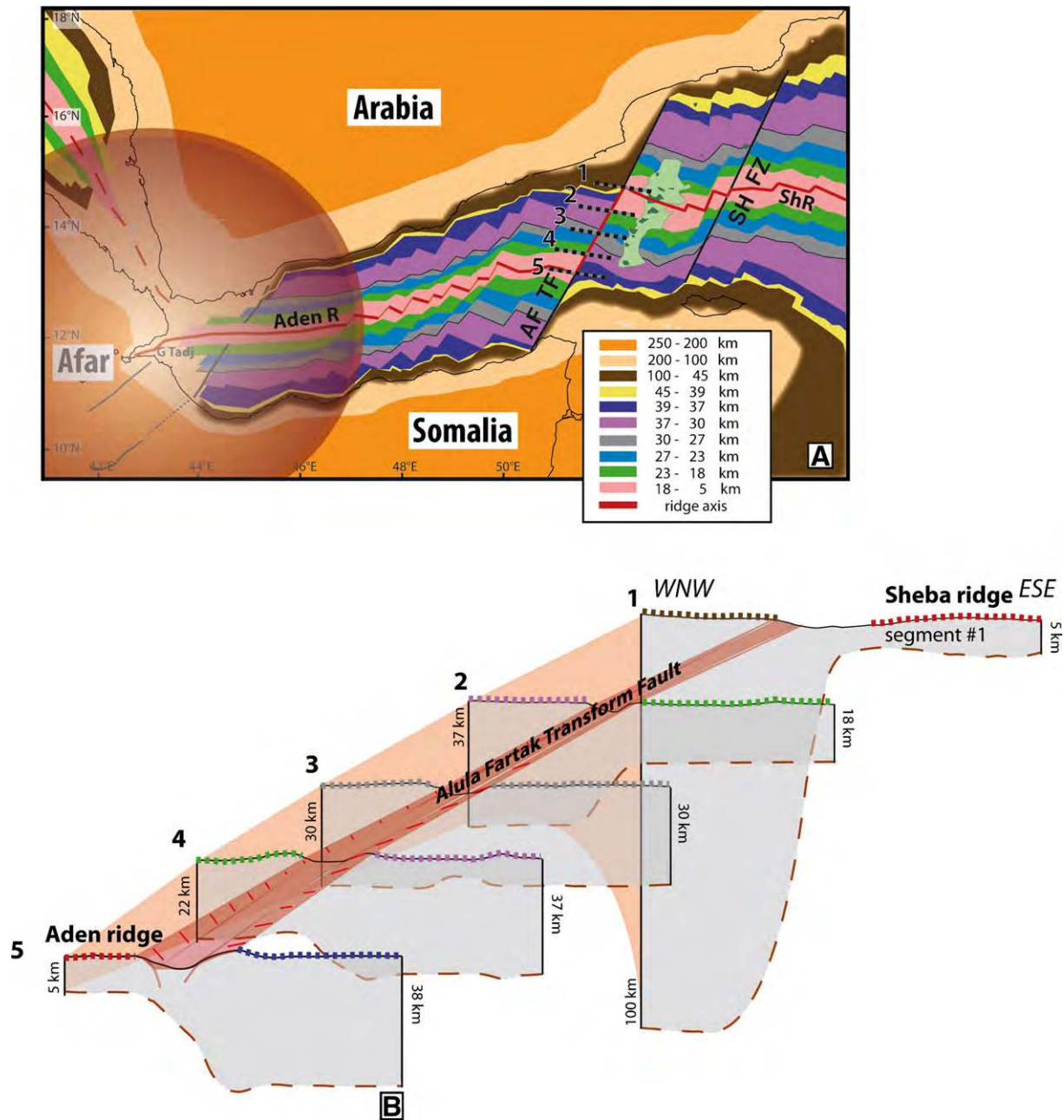
Fig. 9. A — Schematic map of the lithospheric thickness of the Gulf of Aden based on assumption of a half-space cooling model and on the age of the lithosphere with a temperature of 1300 °C (Turcotte and Schubert, 1982). The ages come from the magnetic study in the Gulf of Aden (Leroy et al., 2004; d'Acremont et al., 2006, 2010; this study) and from Bosworth et al. (2005) in the Red Sea. Numbered dashed lines correspond to the location of the cross-sections across the AFTF. See Fig. 2 for the abbreviations of the map. B — Schematic lithospheric cross-sections oriented WNW–ESE crossing the AFTF at five locations. The base of the lithosphere is represented by a dashed brown line. We have drawn on the seafloor a dashed line of colors. Each of the dashed colored lines corresponds to the same color on the lithospheric thickness mapped in the Fig. 9a.

on-axis (Ito et al., 1999) and off-axis (Hall and Kincaid, 2003) plume–ridge systems, could significantly alter plume flow along the Aden and Sheba Ridges. In the case of the on-axis Afar plume system, however, the thick continental lithosphere at the margins of the ocean basin (200 to 250 km) is very close to the spreading axis (between 25 to 200 km) which might enhance the along-axis confinement of plume flow enough to outweigh the effect of a shallow dehydrated layer (Figs. 4d and 9a).

Another particularity of the Afar plume is its location under thick continental lithosphere juxtaposed with relatively thin oceanic lithosphere of the Gulf of Aden and the Red Sea that extend from the Afar hotspot to the east and north respectively. The combination of the Afar plume setting with the narrow newly opened ocean basins each of

which is flanked by thick continental lithosphere may favor channeling of plume material and enhance the along-axis flow (Figs. 8b and 9a). Furthermore, the number of ridge offsets is lower in the western part of the Gulf (offsets are shorter than 50 km), than in the eastern part. Longer transform offset are thought to have a greater the damming effect of the along-axis flow than shorter transform offsets. Plume material flowing along the Aden–Sheba ridge system would not encounter a large offset until it arrives at the AFTF (Figs. 8b and 9a). This 180 km offset might inhibit along-axis flow. Rather than simply damming along-axis flow, long offset transforms may have the effect of redirecting flow along the transform towards the next ridge segment (Georgen and Lin, 2003). Analyses of flux reduction across transform faults show that an offset >300 km should produce a flux reduction of >40% compared to the no-

transform case (Georgen and Lin, 2003). The 180 km offset of the AFTF might reduce along-axis flux by 20%.

Fig. 9b presents the interpreted variations in lithospheric thickness across the AFTF at five schematic cross-sections. These sections show that the lithospheric thickness variability is low from one side of the AFTF to the other within ~15 km of the melting anomaly, suggesting that the plume material channelized below the Aden Ridge may be able to cross the AFTF without complete damming or build up of significant pooling. Lithospheric thickness is about the same on either side of AFTF near the middle of the transform (Fig. 9b section 3). The plume flow may be sufficient to overcome the damming effect of the transform at this location so that along-axis flow of plume material may feed the off-axis melting anomaly on the flanks of the Sheba Ridge. The presence of the four small volcanoes to the west of the melting anomaly (Fig. 3) and the negative RMBA (about −270 mGals) that extends from the AFTF towards the melting anomaly (double arrows in Fig. 6) could be interpreted as observable consequences of this "crossing".

When considering the possibility of channeled along-axis flow, the small offsets of the fracture zones of the Aden Ridge, the narrowness of the oceanic basin and the degree to which the AFTF might impede flow, it is possible to imagine a significant extent of channelized lateral plume flow. If the AFTF also acts as a channel for flow of plume material, flow might conceivably reach the boundary of the continental lithosphere at the northern and southern margins. This may explain recent volcanism west of the AFTF in small onshore areas in Yemen and Somalia.

5. Conclusion

Our analyses of marine geophysical data from the Gulf of Aden point to a period of anomalous heating and associated volcanic activity between AFFZ and SHFZ, from prior to 10 Ma to the present and possibly starting as early as the period immediately following the breakup of Arabia and Africa (~18 Ma). Observations (unusual seafloor morphology; a RMBA low; a low resistivity domain, anomalous mantle seismic structure and geochemical evidence) indicate that previous models, based in part on the limits of extrusive volcanism preserved onshore, which suggest that the SSFZ is the eastern limit of the Afar plume influence, may require re-evaluation and revision (Tard et al., 1991). We propose an Afar plume origin for the melting anomaly interpreted between the AFFZ and the SHFZ of the Sheba Ridge. Hot material coming from the Afar plume is channeled along the corridor formed by the Aden–Sheba ridge system as far eastwards as Yemen, Somalia and Oman (Fig. 8b). The relatively long offset of the AFTF may limit the extent of along-axis flow and redirect small amounts of melt into a flattened lens orientated north–south along the transform, possibly generating onshore volcanoes in Somalia and Yemen. The lithospheric thickness differential across the AFFZ may also allow enhanced melt supply to reach segment 1 of the Sheba Ridge as well as feed the volcanoes on the ridge flanks and onshore. If channeled flow has been ongoing since continental break-up (~18 Ma), when the Aden Ridge was at the same latitude as the southern continental margin in the eastern Gulf of Aden (Fig. 7), then the contrasting lithospheric thickness of the young spreading axis and of the rifted margin may have enhanced channeling. At this time the plume material would have been able to flow away from Afar thanks to the constraining Aden–AFTF–Sheba corridor, feeding the volcanoes located in the ocean–continent transitional domain (Lucazeau et al., 2009). As alternatives to the channeled plume flow model, local fixed mantle source, a source associated with seafloor spreading, and radial plume dispersion were considered as possible explanations, but they fail to fit the observations.

Isotopic geochemical analysis of samples from the volcanoes that have been mapped on the floor of the Gulf of Aden is needed to further constrain the source of the melt that produced them. In addition, it is likely that other volcanoes, not yet mapped, but containing additional clues to the presence and movement of melt beneath the Gulf of Aden, exist. In order to locate these and to further constrain the geometry and viscosity structure of the ridge, full-resolution bathymetry, magnetic, gravity, seismic and electro-magnetic data coverage are needed throughout the Gulf of Aden. Such a study would help to confirm the existence of channelized flow along the Aden and Sheba Ridges and could lead to an estimate of the total plume flux and to better understanding of the effect of transform faults on plume flow in a context of nearby continental margins.

References

Albers, M., Christensen, U.R., 2001. Channeling of plume flow beneath mid-ocean ridges. Earth Planet. Sci. Lett. 187, 207–220.

Audin, L., Manighetti, I., Tapponnier, P., Metivier, F., Jacques, E., Huchon, P., 2001. Fault propagation and climatic control of sedimentation on the Ghoubbet Rift floor; insights from the Tadjouraden cruise in the western Gulf of Aden. Geophys. J. Int. 144, 391–413.

Audin, L., Quidelleur, X., Coulié, E., Courtillot, V., Gilder, S., Manighetti, I., Gillot, P., Tapponnier, P., Kidane, T., 2004. Paleomagnetism and K–Ar and 40Ar/39Ar ages in the Ali Sabieh area (Republic of Djibouti and Ethiopia): constraints on the mechanism of Aden ridge propagation into southeastern Afar during the last 10 Myr. Geophys. J. Int. 158, 327–345.

Autin, J., Leroy, S., Beslier, M.O., d'Acremont, E., Razin, P., Ribodetti, A., Bellahsen, N., Robin, C., Al-Toubi, K., 2010. Continental break-up history of a deep magma-poor margin from seismic reflection data (northeastern Gulf of Aden margin, offshore Oman). Geophys. J. Int. 180, 501–519.

Baker, J., Snee, L., Menzies, M., 1996. A brief Oligocene period of flood volcanism in Yemen: implications for the duration and rate of continental flood volcanism at the Afro-Arabian triple junction. Earth Planet. Sci. Lett. 138, 39–55.

Bastow, I.D., Stuart, G.W., Kendall, J.M., Ebinger, C.J., 2005. Upper-mantle seismic structure in a region of incipient continental breakup: northern Ethiopian rift. Geophys. J. Int. 162, 479–493.

Basuyau, C., Tiberi, C., Leroy, S., Stuart, G., Al-Lazki, A., Al-Toubi, K., Ebinger, C., 2010. Evidence of partial melting beneath a continental margin: case of Dhofar, in the Northern Gulf of Aden (Sultanante of Oman). Geophys. J. Int. 180, 520–534.

Bellahsen, N., Faccenna, C., Funiciello, F., Daniel, J.-M., Jolivet, L., 2003. Why did Arabia separate from Africa? Insights from 3-D laboratory experiments. Earth Planet. Sci. Lett. 216, 365–381.

Bellahsen, N., Fournier, M., d'Acremont, E., Leroy, S., Daniel, J.-M., 2006. Fault reactivation and rift localization: northeastern Gulf of Aden margin. Tectonics 25, 1–14.

Benoit, M.H., Nyblade, A.A., Owens, T.J., Stuart, G., 2006. Mantle transition zone structure and upper mantle S velocity variations beneath Ethiopia: evidence for a broad, deep-seated thermal anomaly. Geochem. Geophys. Geosyst. 7, 1–16.

Bertrand, H., Chazot, G., Blichert-Toft, J., Thoral, S., 2003. Implications of widespread high-[mu] volcanism on the Arabian Plate for Afar mantle plume and lithosphere composition. Chem. Geol. 198, 47–61.

Birse, A.C.R., Bott, W.F., Morrison, J., Samuel, M.A., 1997. The Mesozoic and early Tertiary tectonic evolution of the Socotra area, eastern Gulf of Aden, Yemen. Mar. Petrol. Geol. 14, 675–684.

Bosworth, W., Huchon, P., McClay, K., 2005. The Red Sea and Gulf of Aden basins.; Phanerozoic evolution of Africa. J. Afric Earth Sci. 43, 334–378.

Canales, J.P., Ito, G., Detrick, R.S., Sinton, J., 2002. Crustal thickness along the western Galápagos Spreading Center and the compensation of the Galápagos hotspot swell. Earth Planet. Sci. Lett. 203, 311–327.

Constable, S., Heinson, G., 2004. Hawaiian hot-spot swell structure from seafloor MT sounding. Tectonophysics 389, 111–124.

Coulie, E., Quidelleur, X., Gillot, P.Y., Courtillot, V., Lefevre, J.C., Chiesa, S., 2003. Comparative K–Ar and Ar/Ar dating of Ethiopian and Yemenite Oligocene volcanism: implications for timing and duration of the Ethiopian traps. Earth Planet. Sci. Lett. 206, 477–492.

Courtillot, V., Jaupart, C., Manighetti, I., Tapponnier, P., Besse, J., 1999. On causal links between flood basalts and continental breakup. Earth Planet. Sci. Lett. 166, 177–195.

Courtillot, V., Davaille, A., Besse, J., Stock, J., 2003. Three distinct types of hotspots in the Earth's mantle. Earth Planet. Sci. Lett. 205, 295–308.

d'Acremont, E., 2002. De la déchirure continentale à l'accrétion océanique: ouverture du golfe d'Aden oriental, PhD thesis, 330 pp., Univ. of Paris 6, Paris.

d'Acremont, E., Leroy, S., Beslier, M.O., Bellahsen, N., Fournier, M., Robin, C., Maia, M., Gente, P., 2005. Structure and evolution of the eastern Gulf of Aden conjugate margins from seismic reflection data. Geophys. J. Int. 160, 869–890.

d'Acremont, E., Leroy, S., Maia, M., Patriat, P., Beslier, M.O., Bellahsen, N., Fournier, M., Gente, P., 2006. Structure and evolution of the eastern Gulf of Aden: insights from magnetic and gravity data (Encens–Sheba/MD117 cruise). Geophys. J. Int. 165, 786–803.

d'Acremont, E., Leroy, S., Maia, M., Gente, P., Autin, J., 2010. Volcanism, ridge jump and ridge propagation in the eastern Gulf of Aden: segmentation evolution and implications for accretion processes. Geophys. J. Int. 180, 520–534.

Dauteuil, O., Huchon, P., Quemeneur, F., Souriot, T., 2001. Propagation of an oblique spreading center: the western Gulf of Aden. Tectonophysics 332, 423–442.

Debayle, E., Leveque, J.-J., Cara, M., 2001. Seismic evidence for a deeply rooted low-velocity anomaly in the upper mantle beneath the northeastern Afro/Arabian continent. Earth Planet. Sci. Lett. 193, 423–436.

Douglass, J., Schilling, J.G., Kingsley, R.H., Small, C., 1995. Influence of the discovery and Shona mantle plumes on the southern mid-Atlantic Ridge: rare earth evidence. Geophys. Res. Lett. 22, 2893–2896.

Ebinger, C.J., Sleep, N.H., 1998. Cenozoic magmatism throughout east African resulting from impact of a single plume. Nature 395, 788–791.

Ellis, A.C., Kerr, H.M., Cornwell, C.P., Williams, D.O., 1996. A tectono-stratigraphic framework for Yemen and its implications for hydrocarbon potential. Petrol. Geosci. 2, 29–42.

Fantozzi, P.L., Sgavetti, M., 1998. Tectonic and sedimentary evolution of the eastern Gulf of Aden continental margins: new structural and stratigraphic data from Somalia and Yemen. In: Purser, B.H., Bosence, D.W.J. (Eds.), Sedimentation and Tectonics of Rift Basins: Red Sea-Gulf of Aden. Chapman & Hall, London, pp. 56–76.

Farr, T., Kobrick, M., 2000. Shuttle radar topography mission produces a wealth of data. Eos Trans. 81, 583–585.

Feakins, S.J., Brown, F.H., deMenocal, P.B., 2007. Plio-Pleistocene microtephra in DSDP site 231, Gulf of Aden. J. Afr. Earth Sci. 48, 341–352.

Fisher, R.L., Bunce, E.T., Cernock, P.J., Clegg, D.C., Cronan, D.S., Damiani, V.V., Dmitriev, L.V., Kinsman, D.J., Roth, P.H., Thiede, J., Vincent, E., 1974. Site 231. Initial Reports of the Deep Sea Drilling Project, 24, pp. 17–125.

Fournier, M., Patriat, P., Leroy, S., 2001. Reappraisal of the Arabia–India–Somalia triple junction kinematics. Earth Planet. Sci. Lett. 189, 103–114.

Fournier, M., Petit, C., Chamot-Rooke, N., Fabbri, O., Huchon, P., Maillot, B., Lepvrier, C., 2008. Do ridge–ridge–fault triple junctions exist on Earth? Evidence from the Aden–Owen–Carlsberg junction in the NW Indian Ocean. Basin Res. 20, 575–590.

George, R., Rogers, N., Kelley, S., 1998. Earliest magmatism in Ethiopia; evidence for two mantle plumes in one flood basalt province. Geology 26, 923–926.

Georgen, J.E., Lin, J., Dick, H.J.B., 2001. Evidence from gravity anomalies for interactions of the Marion and Bouvet hotspots with the southwest Indian ridge: effects of transform offsets. Earth Planet. Sci. Lett. 187, 283–300.

Georgen, J.E., Lin, J., 2003. Plume–transform interactions at ultra-slow spreading ridges: implications for the southwest Indian Ridge. Geochem. Geophys. Geosyst. 4, 9106.

Graham, D.W., Johnson, K.T., Douglas Priebe, L., Lupton, J.E., 1999. Hotspot–ridge interaction along the Southeast Indian Ridge near Amsterdam and St. Paul islands: helium isotope evidence. Earth Planet. Sci. Lett. 167, 297–310.

Gregg, P.M., Lin, J., Behn, M.D., Montesi, L.G.J., 2007. Spreading rate dependence of gravity anomalies along oceanic transform faults. Nature 448, 183–187.

Gurnis, M., Mitrovica, J., Ritsema, J., van Heijst, H., 2000. Constraining mantle density structure using geological evidence of surface uplift rates: the case of the African superplume. Geochem. Geophys. Geosyst. 1.

Hall, P.S., Kincaid, C., 2003. Melting, dehydration, and the dynamics of off-axis plume–ridge interaction. Geochem. Geophys. Geosyst. 4, 8510.

Hansen, S.E., Rodgers, A.J., Schwartz, S.Y., Al-Amri, A.M.S., 2007. Imaging ruptured lithosphere beneath the Red Sea and Arabian Peninsula. Earth Planet. Sci. Lett. 259, 256–265.

Hébert, H., Deplus, C., Huchon, P., Khanbari, K., Audin, L., 2001. Lithospheric structure of a nascent spreading ridge inferred from gravity data: the western Gulf of Aden. J. Geophys. Res. 106, 26345–26363.

Hirth, G., Kohlstedt, D., 1996. Water in the oceanic upper mantle: implications for rheology, melt extraction and the evolution of the lithosphere. Earth Planet. Sci. Lett. 144, 93–108.

Hofmann, C., Courtillot, V., Féraud, G., Rochette, P., Yirgu, E., Kefeto, E., Pik, R., 1997. Timing of the Ethiopian flood basalt event and implications for plume birth and global change. Nature 389, 838–841.

Hooft, E.E., Detrick, R.S., Toomey, D.R., Collins, J.A., Lin, J., 2000. Crustal thickness and structure along three contrasting spreading segments of the Mid-Atlantic Ridge, 33.5° –35°N. J. Geophys. Res. 105, 8205–8226.

Ito, G.T., Lin, J., 1995. Mantle temperature anomalies along the past and paleoaxes of the Galápagos spreading center as inferred from gravity analyses. J. Geophys. Res. 100, 3733–3746.

Ito, G., Lin, J., Gable, C., 1996. Dynamics of mantle flow and melting at a ridge centered hotspot: Iceland and the mid-Atlantic Ridge. Earth Planet. Sci. Lett. 144.

Ito, G., Lin, J., Gable, C.W., 1997. Interaction of mantle plumes and migrating mid-ocean ridges: implications for the Galapagos plume–ridge system. J. Geophys. Res. 102.

Ito, G., Shen, Y., Hirth, G., Wolfe, C.J., 1999. Mantle flow, melting, and dehydration of the Iceland mantle plume. Earth Planet. Sci. Lett. 165, 81–96.

Ito, G., Lin, J., Graham, D., 2003. Observational and theoretical studies of the dynamics of mantle plume–mid-ocean ridge interaction. Rev. Geophys. 41, 1017–1040.

Kieffer, B., Arndt, N., Lapierre, H., Bastien, F., Bosch, D., Pecher, A., Yirgu, G., Ayalew, D., Weis, D., Jerram, D.A., Keller, F., Meugniot, C., 2004. Flood and shield basalts from Ethiopia: magmas from the African superswell. J. Petrology 45, 793–834.

Knox, R.P., Nyblade, A.A., Langston, C.A., 1998. Upper mantle S velocities beneath Afar and western Saudi Arabia from Rayleigh wave dispersion. Geophys. Res. Lett. 25, 4233–4236.

Leroy, S., Gente, P., Fournier, M., d'Acremont, E., Patriat, P., Beslier, M.O., Bellahsen, N., Maia, M., Blais, A., Perrot, J., Al-Kathiri, A., Merkouriev, S., Fleury, J.M., Ruellan, P.Y., Lepvrier, C., Huchon, P., 2004. From rifting to spreading in the eastern Gulf of Aden: a geophysical survey of a young oceanic basin from margin to margin. Terra Nova 16, 185–192 doi:10.1111/j.1365-3121.2004.00550.x.

Leroy, S., Ebinger, C., d'Acremont, E., Stuart, G., Al-Lazki, A., Tiberi, C., Autin, J., Watremez, L., Beslier, M.O., Bellahsen, N., Lucazeau, F., Perrot, J., Mouthereau, F., Courrèges, E., Huchon, P., Rouzo, S., Bahalaf, S., Sholan, J., Unternehr, P., Hello, Y., Anglade, A., Desprez, O., Beguery, L., Aouji, O., Daniel, R., Al-Toubi, K., Sage, F., Khanbari, K., 2006. The Onshore–Offshore ENCENS Project: Imaging the Stretching/ Thinning of the Continental Lithosphere and Inception of Oceanic Spreading in the Eastern Gulf of Aden, AGU Fall Meeting, AGU, San Francisco.

Leroy, S., et al., submitted for publication. Contrasted styles of rifting in the eastern Gulf of Aden: a combined wide-angle, MCS and Heat Flow survey. Gcubed, the AGU Fall meeting, December 2009.

Lucazeau, F., Leroy, S., Bonneville, A., Goutorbe, B., Rolandone, F., d'Acremont, E., Watremez, L., Düsünur, D., Tuchais, P., Huchon, P., Bellahsen, N., Al-Toubi, K., 2008. Persistent thermal activity at the Eastern Gulf of Aden after continental break-up. Nature Geosci. 1, 854–858 doi:810.1038/ngeo1359.

Lucazeau, F., Leroy, S., Autin, J., Bonneville, A., Goutorbe, B., Rolandone, F., d'Acremont, E., Watremez, L., Düsünur, D., Tuchais, P., Huchon, P., Bellahsen, N., 2009. Post-rift volcanism and high heat-flow at the ocean–continent transition of the Gulf of Aden. Terra Nova 21, 285–292.

Mahoney, J., Natland, J.H., White, W.M., Poreda, R., Bloomer, S.H., Fisher, R.L., Baxter, A. N., 1989. Isotopic and geochemical provinces of the western Indian Ocean spreading centers. J. Geophys. Res. 94, 4033–4052.

Manighetti, I., Tapponnier, P., Courtillot, V., Gruszow, S., Gillot, P.Y., 1997. Propagation of rifting along the Arabia–Somalia plate boundary: the Gulfs of Aden and Tadjoura. J. Geophys. Res. 102, 2681–2710.

Montelli, R., Nolet, G., Dahlen, F.A., Masters, G., 2006. A catalogue of deep mantle plumes: new results from finite-frequency tomography. Geochem. Geophys. Geosyst. 7, 1–69.

Morgan, W.J., 1978. Rodriguez, Darwin, Amsterdam, ..., a second type of hotspot island. J. Geophys. Res. 83, 5355–5360.

Müller, R.D., Royer, J.-Y., Lawver, L.A., 1993. Revised plate motions relative to the hotspots from combined Atlantic and Indian Ocean hotspot tracks. Geology 21, 275–278.

Orihashi, Y., Haraguchi, S., Ishii, T., Tamaki, K., Al-Khirbash, S., 2003. Petrogenesis of E-type mid-ocean ridge basalts near longitude 46°E, the Gulf of Aden. J. Geogr. 112, 732–749.

Park, Y., Nyblade, A.A., Rodgers, A.J., Al-Amri, A., 2007. Upper mantle structure beneath the Arabian Peninsula and northern Red Sea from teleseismic body wave tomography: implications for the origin of Cenozoic uplift and volcanism in the Arabian Shield. Geochem. Geophys. Geosyst. 8, 1–15.

Pik, R., Marty, B., Hilton David, R., 2006. How many mantle plumes in Africa?; the geochemical point of view.; Special issue in honour of R. K. O'Nions. Chem. Geol. 226, 100–114.

Platel, J.-P., Roger, J., 1989. Evolution géodynamique du Dhofar (Sultanat d'Oman) pendant le Crétacé et le Tertiaire en relation avec l'ouverture du golfe d'Aden. Bull. Soc. Geol. France V (2), 253–263.

Rabain, A., Cannat, M., Escartin, J., Pouliquen, G., Deplus, C., Rommevaux-Jestin, C., 2001. Focused volcanism and growth of a slow spreading segment (Mid-Atlantic Ridge, 35°N). Earth Planet. Sci. Lett. 185, 211–224.

Renkin, M., Sclater, J., 1988. Depth and age in the north Pacific. J. Geophys. Res. 93, 2919–2935.

Ribe, N., Christensen, U.R., Theissing, J., 1995. The dynamics of plume–ridge interaction: 1 Ridge-centered plumes. Earth Planet. Sci. Lett. 134, 155–168.

Ribe, N.M., 1996. The dynamics of plume–ridge interaction 2. Off-ridge plumes. J. Geophys. Res. 101.

Ritsema, van Heijst Hendrik, J., 2000. New seismic model of the upper mantle beneath Africa. Geology (Boulder) 28, 63–66.

Schilling, J.G., Kingsley, R.H., Devine, J.D., 1982. Galapagos hotspot-spreading center system 1. Spatial petrological and geochemical variations (83°W–101°W). J. Geophys. Res. 87.

Schilling, J.G., Zajac, M., Evans, R., Johnston, T., White, W., Devine, J.D., Kingsley, R., 1983. Petrologic and geochemical variations along the Mid-Atlantic Ridge from 29ºN to 73ºN. Am. J. Sci. 283, 510–586.

Schilling, J.G., Thompson, G., Kingsley, R., Humphris, S., 1985. Hotspot–migrating ridge interaction in the South Atlantic. Nature 313, 187–191.

Schilling, J.-G., 1991. Fluxes and excess temperatures of mantle plumes inferred from their interaction with migrating mid-ocean ridges. Nature 352, 397–401.

Schilling, J.-G., Kingsley, R.H., Hanan, B.B., McCully, B.L., 1992. Nd–Sr–Pb isotopic variations along the Gulf of Aden — evidence for Afar mantle plume–continental lithosphere interaction. J. Geophys. Res. 97, 10927–10966.

Sebai, A., Stutzmann, E., Montagner, J.-P., Sicilia, D., Beucler, E., 2006. Anisotropic structure of the African upper mantle from Rayleigh and Love wave tomography. Phys. Earth Planet. Int. 155, 48–62.

13

Sempéré, J.-C., Lin, J., Brown, H.S., Schouten, H., Purdy, G.M., 1993. Segmentation and morphotectonic variations along a slow spreading center: the Mid-Atlantic Ridge (24°00′N–30°40′N). Mar. Geophys. Res. 15, 153–200.

Sicilia, D., Montagner, J.-P., Cara, M., Stutzmann, E., Debayle, E., Lépine, J.-C., Lévêque, J.-J., Beucler, E., Sebai, A., Roult, G., Ayele, A., Sholan, J., 2008. Upper mantle structure of shear-waves velocities and stratification of anisotropy in the Afar Hotspot region. Tectonophysics 462, 164–177.

Simmons, N.A., Forte, A.M., Grand, S.P., 2007. Thermochemical structure and dynamics of the African superplume. Geophys. Res. Lett. 34, 1–5.

Sleep, N.H., 1996. Lateral flow and ponding of starting plume material. J. Geophys. Res. 101, 28065–28083.

Smith, W.H.F., Sandwell, D.T., 1997. Global sea floor topography from satellite altimetry and ship depth soundings. Science 277, 1956–1962.

Tamaki, K., Fujimoto, H., 2001. Outline of the Aden New Century Cruise. R/V Hakuho Maru., Fall meeting, AGU, San Francisco.

Tamsett, D., Searle, R., 1990. Structure of the Alula–Fartak Fracture Zone, Gulf of Aden. J. Geophys. Res. 95, 1239–1254.

Tard, F., Masse, P., Walgenwitz, F., Gruneisen, P., 1991. The volcanic passive margin in the vicinity of Aden, Yémen. BCREDP (Bulletin des Centres de Recherches Exploration Production) 15, 1–9.

Tiberi, C., Leroy, S., d'Acremont, E., Bellahsen, N., Ebinger, C., Al Lazki, A., Pointu, A., 2007. Crustal geometry of the northeastern Gulf of Aden passive margin; localization of the deformation inferred from receiver function analysis. Geophys. J. Int. 168, 1247–1260.

Thibaud, R., Gente, P., Maia, M., 1998. A systematic analysis of the Mid-Atlantic Ridge morphology and gravity between 15°N and 40°N: constraints of the thermal structure. J. Geophys. Res. 103, 24223–24243.

Toh, Hiroaki, 2003. Asymmetric electrical structures beneath Mid-Ocean ridges. J. Geogr. 112, 684–691.

Turcotte, D.L., Schubert, G., 1982. Geodynamics: Applications of Continuum Physics to Geological Problems. John Wiley, New York.

Ukstins, I.A., Renne, P.R., Wolfenden, E., Baker, J., Ayalew, D., Menzies, M., 2002. Matching conjugate volcanic rifted margins: 40Ar/39Ar chrono-stratigraphy of pre- and syn-rift bimodal flood volcanism in Ethiopia and Yemen. Earth Planet. Sci. Lett. 198, 289–306.

Vogt, P.R., 1971. Asthenosphere motion recorded by the ocean floor south of Iceland. Earth Planet. Sci. Lett. 13, 153–160.

Vogt, P.R., Johnson, G.L., 1975. Transform faults and longitudinal flow below the mid-oceanic ridge. J. Geophys. Res. 80, 1399–1428.

Vogt, P.R., 1976. Plumes, subaxial pipe flow, and topography along the mid-ocean ridge. Earth Planet. Sci. Lett. 29, 309–325.

Watchorn, F., Nichols, G.J., Bosence, D.W.J., 1998. Rift-related sedimentation and stratigraphy, southern Yemen (Gulf of Aden). In: Purser, B., Bosence, D. (Eds.), Sedimentation and Tectonics in the Rift Basins Red Sea– Gulf of Aden. Chapman & Hall, London, pp. 165–189.

White, R.S., Bown, J.W., Smallwood, J.R., 1995. The temperature of the Iceland plume and origin of outward-propagating V-shaped ridges. J. Geol. Soc. 152, 1039–1045.

Wolfenden, E., Ebinger, C., Yirgu, G., Renne Paul, R., Kelley Simon, P., 2005. Evolution of a volcanic rifted margin; southern Red Sea. Ethiopia. Geol. Soc. Amer. Bull. 117, 846–864.

Zumbo, V., Feraud, G., Bertrand, H., Chazot, G., 1995. 40Ar/39Ar chronology of tertiary magmatic activity in Southern Yemen during the early Red Sea–Aden rifting. J. Volc. Geoth. Res. 65, 265–279.